Weierstraß-Institut
für Angewandte Analysis und Stochastik

Leibniz-Institut im Forschungsverbund Berlin e. V.

Preprint ISSN 2198-5855

Stability of the higher-order splitting methods for the generalized nonlinear Schrödinger equation

Shalva Amiranashvili[1], Raimondas Čiegis[2]

submitted: December 18, 2023

[1] Weierstrass Institute
Mohrenstr. 39
10117 Berlin
Germany
E-Mail: shalva.amiranashvili@wias-berlin.de

[2] Vilnius Gediminas Technical University
Sauletekio av. 11
10223 Vilnius
Lithuania
E-Mail: raimondas.ciegis@vgtu.lt

No. 3070
Berlin 2023

2020 *Mathematics Subject Classification.* 78A40, 78A60, 91G60.

Key words and phrases. Nonlinear optics, nonlinear fibers, nonlinear Schrödinger equation, generalized nonlinear Schrödinger equation, modulation instability, four-wave mixing, spurious instabilities, splitting methods.

Edited by
Weierstraß-Institut für Angewandte Analysis und Stochastik (WIAS)
Leibniz-Institut im Forschungsverbund Berlin e. V.
Mohrenstraße 39
10117 Berlin
Germany

Fax: +49 30 20372-303
E-Mail: preprint@wias-berlin.de
World Wide Web: http://www.wias-berlin.de/

Stability of the higher-order splitting methods for the generalized nonlinear Schrödinger equation

Shalva Amiranashvili, Raimondas Čiegis

Abstract

The numerical solution of the generalized nonlinear Schrödinger equation by explicit splitting methods can be disturbed by so-called spurious instabilities. They are manifested by the appearance of extraneous spectral peaks which change their position in the frequency domain and disappear with decreasing integration step. The spurious instabilities can coexist with the true physical ones, like modulation instability, in which case they are particularly difficult to detect. We consider an arbitrary multiplicative splitting method and discuss conditions necessary for the absence of spurious instabilities.

1 Physical background

The dynamics of many natural systems can be viewed as the evolution of a modulated weakly nonlinear wave, where the modulation evolves on a much larger time scale than the carrier wave itself [19, 20]. A typical example is an optical pulse that contains many field oscillations and whose envelope slowly evolves in a frame propagating at the carrier group velocity v_{gr}. Slow means slow compared to $2\pi/\omega_0$ for the carrier wave at circular frequency ω_0. Taking advantage of scale separation, one derives a simplified propagation equation for the complex wave amplitude ψ. For example, in the context of nonlinear optical fibers the envelope $\psi = \psi(z,\tau)$ depends on the spatial coordinate z along the fiber and the retarded time $\tau = t - z/v_{\mathsf{gr}}$. The resulting generalized nonlinear Schrödinger equation (GNLSE) refers to the co-moving frame and reads [1]

$$i\partial_z\psi + \mathfrak{D}(\psi) + \gamma|\psi|^2\psi = 0, \qquad \mathfrak{D}(e^{-i\Omega\tau}) = D(\Omega)e^{-i\Omega\tau}. \tag{1}$$

Here γ is a material constant that quantifies the presupposed Kerr nonlinearity. For certainty we will consider γ to be positive, as it is in most cases [4].

The so-called dispersion operator $\mathfrak{D}$ is linear and is described by its characteristic function $D(\Omega)$. The latter has its origin in the dispersion law, a dependence between the wave vector and the frequency of the background carrier fiber mode, $k = \beta(\omega)$. Specifically, the characteristic function describes how $\beta(\omega)$ deviates from a straight line in the vicinity of $\omega = \omega_0$

$$D(\Omega) = \beta(\omega_0+\Omega) - \beta_0 - \beta_1\Omega \quad \text{with} \quad \beta_j = \left.\frac{d^j\beta(\omega)}{d\omega^j}\right|_{\omega=\omega_0}.$$

The characteristic function is usually approximated by a polynomial, which makes $\mathfrak{D}$ a differential operator

$$D(\Omega) = \sum_{j=2}^{J}\frac{\beta_j}{j!}\Omega^j, \quad \mathfrak{D} = \sum_{j=2}^{J}\frac{\beta_j}{j!}(i\partial_\tau)^j. \tag{2}$$

DOI 10.20347/WIAS.PREPRINT.3070 Berlin 2023

The contribution of β_0 and $\beta_1 = v_{\text{gr}}^{-1}$ to the pulse evolution was eliminated in the derivation of Eq. (1) by employing ψ and by changing to the moving frame. The other beta coefficients are assumed to be known up to approximation order J.

A typical problem statement for Eq. (1) is that the input pulse shape is known and its further evolution should be calculated along the fiber: given $\psi(z = 0, \tau)$ one looks for $\psi(z > 0, \tau)$. Physicists say Eq. (1) is unidirectional and z-propagated. The most famous member of the equations family (1) is the optical nonlinear Schrödinger equation with $J = 2$

$$i\partial_z\psi - \frac{\beta_2}{2}\partial_\tau^2\psi + \gamma|\psi|^2\psi = 0, \tag{3}$$

which is integrable [23]. Here, the pulse width in the frequency domain is so small that only β_2 counts in Eq. (2). On the other hand, the further generalization of Eq. (1) is necessary for spectrally broad ultrashort optical pulses to account for nonlinear dispersion and Raman scattering [7]. The paper deals with the numerical solution of the GNLSE (1) by split-step methods.

2 Numerical method

Equation (1) has clearly distinguishable terms of different nature, so a splitting scheme is a natural choice for its solution. Using the simplest Lie-Trotter splitting, one goes from $\psi(z = 0, \tau)$ to $\psi(z = h, \tau)$ in two steps. The nonlinear part of Eq. (1), $\partial_z\psi = i\gamma|\psi|^2\psi$, is solved first on $z \in [0, h]$. The result is used as an initial condition in the solution of the linear part, $\partial_z\psi = i\mathfrak{D}(\psi)$, again on $z \in [0, h]$ and typically employing two fast Fourier transforms. The result of the second step is the required approximation for $\psi(z = h, \tau)$. The entire process is then repeated to get $\psi(z = 2h, \tau)$, and so on [20, 1].

If we write the reduced equations for the linear and nonlinear steps as $\partial_z\psi = B(\psi)$ and $\partial_z\psi = A(\psi)$ respectively, and if we denote the linear and nonlinear evolution operators by e^{hB} and e^{hA}, the splitting approximation can we written as

$$\psi(h, \tau) = e^{h(B+A)}\psi(0, \tau) \approx e^{hB}e^{hA}\psi(0, \tau).$$

Here $e^{h(B+A)}$ represents the full evolution operator for Eq. (1). Alternatively, the calculation can start with the linear step followed by the nonlinear step. Unless otherwise stated, we start with the nonlinear step.

While the Lie-Trotter splitting is easy to implement, it still has its drawbacks. Its local accuracy is $O(h^2)$, indicating that the solution method is of first order. The accuracy can be improved by employing a higher order splitting scheme. A general multiplicative splitting method, comprising of n stages, with each stage consisting of a single nonlinear and linear step, is defined by the approximation [14]

$$e^{h(B+A)} \approx e^{b_n hB}e^{a_n hA} \ \cdots \ e^{b_2 hB}e^{a_2 hA}e^{b_1 hB}e^{a_1 hA}, \tag{4}$$

where the last step may be trivial, i.e., b_n may be zero. The coefficients $a_{1\le s\le n}$ and $b_{1\le s\le n}$ are chosen such that the formal Taylor expansions of the left- and right-hand-side of Eq. (4) coincide as good as possible. For instance, the well-known Suzuki-Yoshida splitting [17, 21] has 4 stages and a local accuracy of $O(h^5)$, it provides a fourth-order method. Equation (4) can be easily understood for square matrices. Its relevance to the GNLSE, where the nonlinear operator A is combined with the unbounded linear differential operator B, is discussed in Ref. [20]. Web page [3] includes a compilation of helpful splittings.

Another drawback of splitting methods is that they may suffer from numerical instabilities due to their explicit nature. In the context of GNLSE, these instabilities are known to as the spurious instabilities [6, 13]. Weideman and Herbst [18] tackled this problem by exploiting the well-established physical phenomenon of (non-spurious) modulation instability [22] (MI). Namely, they considered an exact solution to Eq. (3) for the constant-amplitude carrier wave

$$\psi = \sqrt{P_0} e^{i\gamma P_0 z}, \qquad P_0 = \text{const}, \tag{5}$$

which may ($\beta_2\gamma < 0$) or may not ($\beta_2\gamma > 0$) be prone to MI [20, 1]. Weideman and Herbst investigated to what extent this behavior is replicated by the Lie-Trotter splitting method and derived the necessary condition for the absence of spurious instabilities

$$h < \frac{2\pi}{|\beta_2|\Omega_{\text{max}}^2}. \tag{6}$$

Here h is the numerical solution step and the spectrum of $\psi(z,\tau)$ is assumed to have a finite bandwidth, $|\Omega| < \Omega_{\text{max}} = \pi/\Delta\tau$, where $\Delta\tau$ is the discretization step of the "coordinate" τ .

The method that leads to Eq. (6) can be generalized in several directions. One could (i) explore other solutions of the integrable Eq. (3), (ii) consider the more general Eq. (1), which serves as a standard model in nonlinear fiber optics, and (iii) explore an arbitrary splitting.

The first [11, 12] and second [12, 16] approaches have been discussed in the literature, while for the third approach we are only aware on studies of the Suzuki-Yoshida splitting method [20]. In the following, we will discuss the spurious instabilities in regard to Eq. (1) and an arbitrary splitting method.

3 Modulation instability

This section presents essential information regarding MI, which must be accurately reproduced by a numerical solution of Eq. (1). For the full description the reader should consult standard textbooks [20, 1]. We consider a specific subset of solutions to Eq. (1)

$$\psi(z,\tau) = \left(\sqrt{P_0} + \widetilde{\psi}(z,\tau)\right) e^{i(D(\nu)+\gamma P_0)z - i\nu\tau}, \quad \text{where} \quad |\widetilde{\psi}| \ll \sqrt{P_0}. \tag{7}$$

For $\widetilde{\psi} = 0$, Eq. (7) yields an exact solution to Eq. (1). The solution describes a wave with a constant amplitude $\sqrt{P_0}$, its laboratory frequency is $\omega_0 + \nu$. Note, that γP_0 is the nonlinear wave vector shift. In what follows, the dimensionless value of $h\gamma P_0$ will play an important role for a numerical solution with the evolution step h.

The most natural selection in Eq. (7) is $\nu = 0$, bringing us back to the solution (5). Waves with non-zero ν can occur due to inaccurate carrier frequency selection, when several waves with slightly different frequencies are described by one envelope equation, or due to various physical phenomena such as nonlinear waves interactions [10] and self-frequency shift [9, 15]. This holds particularly true for the optical supercontinuum state [8].

With a small but non-zero $\widetilde{\psi}$, we can study the stability of the carrier wave. Equations (1) and (7) yield a linear equation

$$i\partial_z\widetilde{\psi} + e^{i\nu\tau}\mathfrak{D}(\widetilde{\psi}e^{-i\nu\tau}) - D(\nu)\widetilde{\psi} + \gamma P_0(\widetilde{\psi} + \widetilde{\psi}^*) = 0, \tag{8}$$

which has a collection of partial solution that are parameterized by real Ω

$$\widetilde{\psi}(z,\tau) = u(z)e^{-i\Omega\tau} + v^*(z)e^{i\Omega\tau}. \tag{9}$$

From a physical standpoint, two additional waves arise at $\omega = \omega_0 + \nu \pm \Omega$. They are identified as the blue- and red-shifted MI satellites and in accord with Eq. (8) can be found from the system

$$\partial_z \begin{bmatrix} u \\ v \end{bmatrix} = i \begin{bmatrix} N_\nu(\Omega) + M_\nu(\Omega) + \gamma P_0 & \gamma P_0 \\ -\gamma P_0 & N_\nu(\Omega) - M_\nu(\Omega) - \gamma P_0 \end{bmatrix} \begin{bmatrix} u \\ v \end{bmatrix}. \tag{10}$$

Here we introduced notations

$$M_\nu(\Omega) = \frac{D(\nu+\Omega) - 2D(\nu) + D(\nu-\Omega)}{2}, \qquad N_\nu(\Omega) = \frac{D(\nu+\Omega) - D(\nu-\Omega)}{2}, \tag{11}$$

which bear some resemblance to the definitions of discrete derivatives. $M_\nu(\Omega)$ is referred to as mismatch. The matrix in Eq. (10) has eigenvalues $iN_\nu(\Omega) \pm \sqrt{-M_\nu(\Omega)(M_\nu(\Omega) + 2\gamma P_0)}$ and MI takes place if

$$M_\nu(\Omega)(M_\nu(\Omega) + 2\gamma P_0) < 0 \quad \Rightarrow \quad M_\nu(\Omega) \in (-2\gamma P_0, 0), \tag{12}$$

where the final implication uses $\gamma > 0$. In a favorable situation (e.g., for $D''(\nu) < 0$), Eq. (12) yields one or several domains on Ω axis, the domains are translated into growing perturbations (9) indicating presence of the instability. The numerical solution should display these domains up to some approximation, moreover, it should not display any additional domains.

4 Split step approach to modulation instability

To facilitate a comparison between the continuous and discrete solutions, we follow [16] and rephrase the well-known results from the previous section. Equation (10) and its solution are written in the matrix form

$$\partial_z \begin{bmatrix} u \\ v \end{bmatrix} = i(N_\nu(\Omega)\mathbf{I} + M_\nu(\Omega)\mathbf{J} + \gamma P_0 \mathbf{K}) \begin{bmatrix} u \\ v \end{bmatrix}, \quad \begin{bmatrix} u(z) \\ v(z) \end{bmatrix} = e^{iz(N_\nu(\Omega)\mathbf{I} + M_\nu(\Omega)\mathbf{J} + \gamma P_0 \mathbf{K})} \begin{bmatrix} u(0) \\ v(0) \end{bmatrix}, \tag{13}$$

where

$$\mathbf{I} = \begin{bmatrix} 1 & 0 \\ 0 & 1 \end{bmatrix}, \quad \mathbf{J} = \begin{bmatrix} 1 & 0 \\ 0 & -1 \end{bmatrix}, \quad \mathbf{K} = \begin{bmatrix} 1 & 1 \\ -1 & -1 \end{bmatrix}.$$

For an integration step, we have the following exact expression

$$\begin{bmatrix} u(z+h) \\ v(z+h) \end{bmatrix} = e^{ihN_\nu(\Omega)} e^{ih(M_\nu(\Omega)\mathbf{J} + \gamma P_0 \mathbf{K})} \begin{bmatrix} u(z) \\ v(z) \end{bmatrix}. \tag{14}$$

Note, that the determinant of $e^{ih(M_\nu(\Omega)\mathbf{J} + \gamma P_0 \mathbf{K})}$ is 1 and therefore the instability condition is

$$\left| \mathrm{Tr}\left(e^{ih(M_\nu(\Omega)\mathbf{J} + \gamma P_0 \mathbf{K})} \right) \right| > 2. \tag{15}$$

It is not difficult to get $e^{ih(M_\nu(\Omega)\mathbf{J} + \gamma P_0 \mathbf{K})}$ explicitly, which brings Eq. (15) back to the criterion (12).

The above approach can be used with any splitting method. Indeed, Eq. (13) contains terms that come from linear and nonlinear parts of GNLSE. By treating them separately, we see that an arbitrary splitting (4) corresponds to the following approximation

$$\begin{bmatrix} u(z+h) \\ v(z+h) \end{bmatrix} \approx e^{ihN_\nu(\Omega)} \left(\prod_{n \geq s \geq 1} e^{ib_s h M_\nu(\Omega)\mathbf{J}} e^{ia_s h \gamma P_0 \mathbf{K}} \right) \begin{bmatrix} u(z) \\ v(z) \end{bmatrix}. \tag{16}$$

The difference between the exact solution (14) and its approximation (16) appears because $\mathbf{JK} \neq \mathbf{KJ}$. Determinant of the matrix product in Eq. (16) is still 1, such that the inequality

$$\left| \mathrm{Tr} \left(\prod_{n \geq s \geq 1} e^{ib_s h M_\nu(\Omega) \mathbf{J}} e^{ia_s h \gamma P_0 \mathbf{K}} \right) \right| > 2, \tag{17}$$

is the split-step approximation of the MI condition (15).

To proceed with Eq. (17), it is convenient to introduce two dimensionless parameters

$$\varepsilon = h\gamma P_0, \quad \phi = h M_\nu(\Omega). \tag{18}$$

In fiber optics, the quantity $(\gamma P_0)^{-1}$ is referred to as nonlinear length and indicates the propagation distance at which nonlinear effects become significant [1]. In any case, the numerical solution step h should be smaller than the nonlinear length and therefore Eq. (17) can be simplified using $\varepsilon \ll 1$. On the other hand, the value of ϕ can be arbitrary, because "small" h is multiplied by a polynomial $M_\nu(\Omega)$ with possibly "large" Ω. In addition, we introduce the notations

$$b_{pq} = \begin{cases} b_{p-1} + b_{p-2} + \cdots + b_q & \text{if } p > q, \\ 1 - b_{qp} & \text{if } p < q, \end{cases} \qquad \text{and} \qquad \sum_{p,q,\ldots r}{}' = \sum_{p>q>\cdots>r}, \tag{19}$$

where all summation indices in the last expression take all possible values from n to 1 subject to the specified inequality. The trace in Eq. (17) is calculated in the Appendix A, the result reads

$$\begin{aligned} \mathrm{Tr} \left(\prod_{n \geq s \geq 1} e^{ib_s \phi \mathbf{J}} e^{ia_s \varepsilon \mathbf{K}} \right) = {} & 2\cos(\phi) \\ & - 2\varepsilon \sin(\phi) \\ & + 4\varepsilon^2 \sum_{p,q}{}' a_p a_q \sin(b_{pq}\phi) \sin(b_{qp}\phi) \\ & - 8\varepsilon^3 \sum_{p,q,r}{}' a_p a_q a_r \sin(b_{pq}\phi) \sin(b_{qr}\phi) \sin(b_{rp}\phi) \\ & + 16\varepsilon^4 \sum_{p,q,r,s}{}' a_p a_q a_r a_s \sin(b_{pq}\phi) \sin(b_{qr}\phi) \sin(b_{rs}\phi) \sin(b_{sp}\phi) + \cdots . \end{aligned} \tag{20}$$

Applications of this result will be given in the next section. Splitting methods that start with a linear step are discussed in the Appendix B.

5 Examples

Equations (17) and (20) represent the primary outcome of the paper and make it possible to analyze the interplay of the MI and spurious instabilities. Note, that they were obtained by going from $\psi(z, \tau)$ to $\psi(z+h, \tau)$ by an arbitrary splitting method, where the τ variable still is continuous. We will now examine this situation in more detail, and discuss what happens due to the discretization of the retarded time.

True MI Recall that $\varepsilon > 0$ is a small parameter, while ϕ does not have to be small, as discussed after Eq. (18). If nevertheless we consider the case that $\phi = O(\epsilon)$, Eq. (17) yields $|2 - \phi(\phi + 2\varepsilon) + O(\varepsilon^4)| > 2$. This is compatible with the MI condition (12), which translates into $\phi(\phi + 2\varepsilon) < 0$. The resulting MI domain $\phi \in (-2\varepsilon, 0)$ is compatible with the assumption that $\phi = O(\epsilon)$. Therefore the core MI is correctly described by any splitting method. An arbitrary ϕ is another story, this is where the spurious instabilities occur.

Lie-Trotter and Strang splittings For both $e^{h(B+A)} \approx e^{hB}e^{hA}$ (Lie-Trotter) and $e^{h(B+A)} \approx e^{\frac{h}{2}A}e^{hB}e^{\frac{h}{2}A}$ (Strang) splitting methods, the instability condition (17) reduces to

$$|\cos(\phi) - \varepsilon \sin(\phi)| > 1.$$

The inequality also applies to the Lie-Trotter and Strang methods that begin with a linear step. It was first derived in the pioneer paper [18]. The function on the left-hand-side takes its maximal value $\sqrt{1+\varepsilon^2}$ for

$$\phi = \phi_m = \pi m - \arctan\varepsilon, \quad m \in \mathbb{Z}.$$

Each such ϕ_m is in the middle of its instability domain

$$I_m = (\pi m - 2\arctan\varepsilon, \pi m).$$

The true MI domain (12), which is $\phi \in (-2\varepsilon, 0)$, is approximately recovered for $m = 0$, as expected from the previous subsection. The remaining domains are associated with spurious instabilities and there are two obvious ways to remove them.

First, any discrete approximation of $\psi(z = nh, \tau)$ has a finite bandwidth. The inequality $|\Omega| < \Omega_{\text{max}}$ translates into estimating the polynomial mismatch $M_\nu(\Omega)$ and then into an estimate for $\phi = hM_\nu(\Omega)$. The range of the possible ϕ values should be chosen so that it includes I_0 and has no intersections with $I_{\pm 1}$. This is achieved by decreasing h and leads to the classical condition (6). Applications of this approach to GNLSE were discussed in [12, 16]. Another possibility is to study whether the spurious instability domains can be removed by a more accurate splitting method using the general criterion (17). This will be done bellow.

A generic two-stage splitting Consider the approximation

$$e^{h(A+B)} \approx e^{hb_2B}e^{ha_2A}e^{hb_1B}e^{ha_1A}, \quad a_1 + a_2 = 1, \quad b_1 + b_2 = 1.$$

Its local accuracy is $O(h^2)$, it increases up to $O(h^3)$ if $a_2b_1 = 1/2$. Strang splitting belongs to this class, as well as the best-two-stage splitting

$$a_1 = b_2 = 1 - \frac{\sqrt{2}}{2}, \quad a_2 = b_1 = \frac{\sqrt{2}}{2},$$

and rational Milne splitting

$$a_1 = \frac{3}{8}, \quad a_2 = \frac{5}{8}, \quad b_1 = \frac{4}{5}, \quad b_2 = \frac{1}{5},$$

see [3]. Using Eq. (20), one derives the inequality

$$|\cos(\phi) - \varepsilon\sin(\phi) + 2a_1a_2\varepsilon^2\sin(b_1\phi)\sin(b_2\phi)| > 1,$$

where in addition to the true MI that occurs for $\phi = O(\varepsilon)$, it is easy to see that the spurious instabilities are still present in the vicinity of $\phi = \pm\pi$. For a trivial two-stage splitting $e^{\frac{h}{2}B}e^{\frac{h}{2}A}e^{\frac{h}{2}B}e^{\frac{h}{2}A}$, they appear in the vicinity of $\phi = \pm 2\pi$, because the integration step h is actually halved.

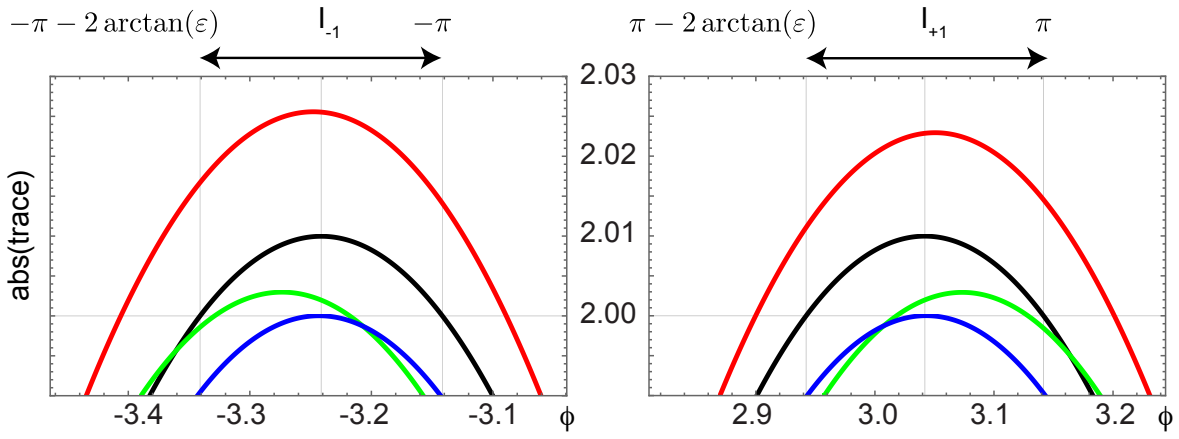

Figure 1: Left-hand-side of Eq. (17) is shown upon $\phi \in I_{-1}$ (left panel) and $\phi \in I_1$ (right panel) for $\varepsilon = 0.1$ and several popular splitting methods. The spurious instabilities appear where $|\text{trace}| > 2$. The following methods are presented: Lie-Trotter (black, the same line for the Strang splitting), Suzuki-Yoshida (red), Suzuki-Yoshida starting with the linear step (green), and S_6 splitting reported by Blanes and Moan [5] (blue, practically the same line for their S_{10} splitting). The latter method seems to be free of the spurious instabilities, but actually has an eigenvalue that exceed 1 to a small amount ($\lambda - 1 \sim 4 \cdot 10^{-3}$ for S_6 and $2 \cdot 10^{-4}$ for S_{10}).

Higher-order splittings Now we consider two practically relevant 4-th order splittings with 6 and 10 stages, S_6 and S_{10} from [5]. As the analytical approach seems to be impossible here, the left-hand-side of Eq. (17) is numerically plotted in Fig. 1. In addition, we show the results for the classical Suzuki-Yoshida splitting [20]. The latter is even worse that the simplest Lie-Trotter method when one starts with a nonlinear step. As to S_6 and S_{10} splittings, the spurious instabilities are strongly suppressed for both of them, but they still exist in extremely narrow domains at $\phi = \pm\pi$.

6 Conclusions

As explained when analyzing the Lie-Trotter and Strang splittings in Section 5, a sure way to eliminate the spurious instabilities is to impose a restriction onto the mismatch (11). Roughly speaking, it is necessary that $h|M_\nu(\Omega)| < \pi$, for all carrier offsets ν and all satellite offsets Ω, for more details see [12, 16]. Using more and more accurate splitting schemes, one still faces the spurious instabilities (Fig. 1). As the approximation order increases, the instabilities tend to become less pronounced, moreover their domain may become extremely narrow, as it happens for the S_6 and S_{10} splittings from [5]. In practice, there are good chances that discrete numerical frequencies does not hit the unstable domain, or that the spurious instability will not have time to develop on a finite integration interval. Nevertheless, the spurious instabilities are present. This leads to a conclusion, that a higher-order splitting can be used to make calculations more accurate with the same h, but it cannot be used to make calculations more fast by employing a considerably larger h. To avoid this trap, the derivation of splitting schemes should be reconsidered. One should take care that the trace in Eq. (17) do not exceed 2 when choosing coefficients of a splitting method. We can hope that it is possible, e.g., because for a trivial two-stage splitting $e^{\frac{h}{2}B}e^{\frac{h}{2}A}e^{\frac{h}{2}B}e^{\frac{h}{2}A}$, which is used in certain additive schemes [2], the spurious instabilities first appear at $h|M_\nu(\Omega)| \approx 2\pi$. One should look for new higher-order splittings with the same property. This will be a topic for future research.

A Trace calculation

In the appendix we outline how Eq. (20) was derived. To this end we consider the matrix from Eq. (17) using notations from Eq. (18)

$$\mathbf{U} = \prod_{n\geq s\geq 1} e^{ib_s\phi\mathbf{J}} e^{ia_s\varepsilon\mathbf{K}} = \begin{bmatrix} e^{ib_n\phi} & 0 \\ 0 & e^{-ib_n\phi} \end{bmatrix} (\mathbf{I} + ia_n\varepsilon\mathbf{K}) \cdot \\ \begin{bmatrix} e^{ib_{n-1}\phi} & 0 \\ 0 & e^{-ib_{n-1}\phi} \end{bmatrix} (\mathbf{I} + ia_{n-1}\varepsilon\mathbf{K}) \cdots \begin{bmatrix} e^{ib_1\phi} & 0 \\ 0 & e^{-ib_1\phi} \end{bmatrix} (\mathbf{I} + ia_1\varepsilon\mathbf{K}) \,.$$

Calculating $\mathbf{U}$, it is natural to introduce an expansion

$$\mathbf{U} = \begin{bmatrix} e^{i\phi} & 0 \\ 0 & e^{-i\phi} \end{bmatrix} + \varepsilon\mathbf{U}^{(1)} + \varepsilon^2\mathbf{U}^{(2)} + \cdots \,,$$

because in all practically relevant cases $\varepsilon \ll 1$, as explained after Eq. (18). We have the following expressions

$$\mathbf{U}^{(1)} = \sum_{n\geq p\geq 1} \begin{bmatrix} e^{i(b_n+\cdots b_p)\phi} & 0 \\ 0 & e^{-i(b_n+\cdots b_p)\phi} \end{bmatrix} (ia_p\mathbf{K}) \begin{bmatrix} e^{i(b_{p-1}+\cdots b_1)\phi} & 0 \\ 0 & e^{-i(b_{p-1}+\cdots b_1)\phi} \end{bmatrix},$$

and

$$\mathbf{U}^{(2)} = \sum_{n\geq p>q\geq 1} \begin{bmatrix} e^{i(b_n+\cdots b_p)\phi} & 0 \\ 0 & e^{-i(b_n+\cdots b_p)\phi} \end{bmatrix} (ia_p\mathbf{K}) \cdot \\ \begin{bmatrix} e^{i(b_{p-1}+\cdots b_q)\phi} & 0 \\ 0 & e^{-i(b_{p-1}+\cdots b_q)\phi} \end{bmatrix} (ia_q\mathbf{K}) \begin{bmatrix} e^{i(b_{q-1}+\cdots b_1)\phi} & 0 \\ 0 & e^{-i(b_{q-1}+\cdots b_1)\phi} \end{bmatrix},$$

with the evident structure of the further terms. Using a cyclic permutation of the first multiplier and the shortcuts from Eq. (19), we see that as long as only traces of the above matrices are of interest, it is possible to make the following replacements

$$\mathbf{U}^{(1)} \mapsto \sum_{n\geq p\geq 1} (ia_p\mathbf{K}) \begin{bmatrix} e^{i\phi} & 0 \\ 0 & e^{-i\phi} \end{bmatrix},$$

$$\mathbf{U}^{(2)} \mapsto \sum_{p,q}{}' (ia_p\mathbf{K}) \begin{bmatrix} e^{ib_{pq}\phi} & 0 \\ 0 & e^{-ib_{pq}\phi} \end{bmatrix} (ia_q\mathbf{K}) \begin{bmatrix} e^{ib_{qp}\phi} & 0 \\ 0 & e^{-ib_{qp}\phi} \end{bmatrix},$$

$$\mathbf{U}^{(3)} \mapsto \sum_{p,q,r}{}' (ia_p\mathbf{K}) \begin{bmatrix} e^{ib_{pq}\phi} & 0 \\ 0 & e^{-ib_{pq}\phi} \end{bmatrix} (ia_q\mathbf{K}) \begin{bmatrix} e^{ib_{qr}\phi} & 0 \\ 0 & e^{-ib_{qr}\phi} \end{bmatrix} (ia_r\mathbf{K}) \begin{bmatrix} e^{ib_{rp}\phi} & 0 \\ 0 & e^{-ib_{rp}\phi} \end{bmatrix},$$

and so on. With the help of some computer algebra, traces of the latter expressions finally lead to the expansion (20).

B Splitting methods that start with a linear step

Recall, that the linear and nonlinear evolution operators were denoted by e^{hB} and e^{hA}, so a generic splitting method (4) starts with a nonlinear step. If one chooses to start with a linear step, Eq. (4) should be replaced by

$$e^{h(B+A)} \approx e^{b_nhA}e^{a_nhB} \,\cdots\, e^{b_2hA}e^{a_2hB}e^{b_1hA}e^{a_1hB}, \tag{21}$$

and the reformulated Eq. (17) is

$$\left|\mathrm{Tr}\left(\prod_{n\geq s\geq 1} e^{ib_s h\gamma P_0 \mathbf{K}} e^{ia_s h M_\nu(\Omega)\mathbf{J}}\right)\right| > 2.$$

The latter inequality gets the same structure as the original Eq. (17) after a cyclic permutation that moves the last exponent to the first place, the trace is not affected. Therefore we can take any relation derived from Eq. (17), apply the replacement rule

$$b_n, a_n, b_{n-1}, a_{n-1} \cdots b_2, a_2, b_1, a_1 \quad \mapsto \quad a_1, b_n, a_n, b_{n-1} \cdots a_3, b_2, a_2, b_1,$$

and get the linked result for the splitting method (21). The practical difference between the splittings (4) and (21) can be quite significant, see Fig. 1.

References

[1] G. P. Agrawal. *Nonlinear Fiber Optics*. Academic, New York, 4 edition, 2007.

[2] Sh. Amiranashvili, M. Radziunas, U. Bandelow, K. Busch, and R. Čiegis. Additive splitting methods for parallel solutions of evolution problems. *Journal of Computational Physics*, 436(110320):1–14, July 2021.

[3] W. Auzinger, H. Hofstätter, and O. Koch. Coefficients of various splitting methods. `https://www.asc.tuwien.ac.at/~winfried/splitting/`.

[4] M. Bass, E. W. Van Stryland, D. R. Williams, and W. L. Wolfe, editors. *Handbook of Optics*, volume 1. McGRAW-HILL, 2 edition, 1995.

[5] S. Blanes and P. C. Moan. Practical symplectic partitioned Runge-Kutta and Runge-Kutta-Nyström methods. *Journal of Computational and Applied Mathematics*, 142(2):313–330, May 2002.

[6] G. Bosco, A. Carena, V. Curri, R. Gaudino, P. Poggiolini, and S. Benedetto. Suppression of spurious tones induced by the split-step method in fiber systems simulation. *IEEE Photonics Technology Letters*, 13(5):489–491, May 2000.

[7] R. W. Boyd. *Nonlinear Optics*. Academic, New York, 3 edition, 2008.

[8] J. M. Dudley, G. Genty, and S. Coen. Supercontinuum generation in photonic crystal fiber. *Rev. Mod. Phys.*, 78(4):1135–1184, 2006.

[9] J. P. Gordon. Theory of the soliton self-frequency shift. *Opt. Lett.*, 11(10):662–664, October 1986.

[10] E. Kartashova. *Nonlinear Resonance Analysis*. Cambridge University Press, 2010.

[11] T. I. Lakoba. Instability analysis of the split-step Fourier method on the background of a soliton of the nonlinear Schrödinger equation. *Numerical Methods for Partial Differential Equations*, 28(2):641–669, March 2012.

[12] T. I. Lakoba. Instability of the split-step method for a signal with nonzero central frequency. *J. Opt. Soc. Am. B*, 30(12):3260–3271, December 2013.

[13] T. I. Lakoba. Long-time simulations of nonlinear Schrödinger-type equations using step size exceeding threshold of numerical instability. *J Sci Comput*, 72(1):14–48, July 2017.

[14] R.I. McLachlan and R. Quispel. Splitting methods. *Acta Numerica*, 11:341–434, January 2002.

[15] F. M. Mitschke and L. F. Mollenauer. Discovery of the soliton self-frequency shift. *Opt. Lett.*, 11(10):569–661, 1986.

[16] F. Severing, U. Bandelow, and Sh. Amiranashvili. Spurious four-wave mixing processes in generalized nonlinear schrödinger equations. *J. Lightwave Technol.*, 41(16):5359–5365, August 2023.

[17] M. Suzuki. Fractal decomposition of exponential operators with applications to many-body theories and Monte Carlo simulations. *Phys. Lett. A*, 146(6):319–323, June 1990.

[18] J. A. C. Weideman and B. M. Herbst. Split-step methods for the solution of the nonlinear Schrödinger equation. *SIAM J. Numer. Anal.*, 23(3):485–507, June 1986.

[19] G. B. Whitham. *Linear and nonlinear waves*. John Wiley & Sons, New York, 1974.

[20] J. Yang. *Nonlinear Waves in Integrable and Nonintegrable Systems*. SIAM, 2010.

[21] H. Yoshida. Construction of higher order symplectic integrators. *Phys. Lett. A*, 150(5-7):262–268, November 1990.

[22] V. E. Zakharov and L. A. Ostrovsky. Modulation instability: the beginning. *Physica D: Nonlinear Phenomena*, 238(5):540–548, March 2009.

[23] V. E. Zakharov and A. B. Shabat. Exact theory of two-dimensional self-focusing and one-dimensional self-modulation of waves in nonlinear media. *Sov. Phys. JETP*, 34(1):62–69, 1972.